Electron Traps and the Stark Effect on Hydroxylated Titania Photocatalysts

Steven H. Szczepankiewicz,† John A. Moss, and Michael R. Hoffmann*

W. M. Keck Laboratories, California Institute of Technology, Pasadena, California 91125

Received: February 20, 2002; In Final Form: May 20, 2002

Electric fields generated by photoexcited charge carriers in TiO_2 (anatase) produce Stark effect intensity and wavelength shifts for surface TiO−H stretching vibrations. Deep electron-trapping states affect a single type of TiO−H stretch (Ti(IV)O−H at 3647 cm^{-1} ⇒ Ti(III)O−H at 3716 cm^{-1}). Shallow electron-trapping states, observed as broad absorption bands above 3000 cm^{-1}, produce an apparently homogeneous electric field. Intensity changes and corresponding wavelength shifts for ν(TiO−H) are proportional to the magnitude and polarity of the electric field. O_2 is shown to reversibly abstract electrons from shallow trapping states. The results suggest that shallow electron traps are not associated with localized structures, but rather are delocalized across the TiO_2 surface. This behavior may explain the photon-dependent wettability of TiO_2 surfaces.

Introduction

Photoactivated TiO_2 is commonly used to assist the total oxidation of aqueous and vapor-phase organic pollutants.[1] Low conversion efficiency prevents the industrial-scale implementation of photocatalytic decontamination processes. Charge carrier recombination, which limits efficiency, is minimized when the charges are spatially separated. Band gap irradiation of TiO_2 promotes electrons from the valence band to the conduction band, forming an electron−hole pair. Charge separation of the exciton pair is achieved by immobilizing one or both charges in mid band-gap traps.[2] The holes, which have a relatively small effective mass and high oxidizing potential (+3.0 V vs NHE), are readily trapped at the semiconductor surface by oxidizing surface-bound hydroxyl groups to hydroxyl radicals, or by oxidizing lattice oxygen from the −2 to 0 valence state and thereby creating an oxygen vacancy. Electrons, on the other hand, have a higher effective mass and moderate reduction potential (−0.2 V vs NHE) that allows them to remain in either the free state or to be trapped at the surface. Surface electron traps, which lower the potential of the CB electron, are defined as shallow if they lie above the reduction potential of O_2. Within seconds after irradiation, in the absence of external electron donors or acceptors, illuminated TiO_2 contains holes trapped as hydroxyl radicals and oxygen vacancies, along with electrons that are deeply trapped, shallowly trapped, and freely mobile, each with a distinct spectral response in the infrared.

Charge separation due to trapping in TiO_2 produces an electric field that can be observed as a bulk effect[3] and by its molecular influence.[4] Electric fields affect semiconductor photodynamics when the splitting of one exciton pair causes a Stark effect on the absorption of a second pair.[2,5] The Stark effect characterizes the influence of an electric field on spectroscopic transitions, which are commonly manifested as intensity and wavelength shifts. For electronic transitions, the Stark wavelength dependence (Stark tuning rate) is the result of changing the relative potentials of the initial and/or final states, while the intensity shifts are apparent through changes in transition oscillator strength. For vibrational spectroscopy, these changes are manifested as structural modifications as the oscillating dipole responds to the electric field, changing bond lengths and orbital overlap. When the vibrational Stark effect is well-described for a system, either the dipole moment of the vibrating molecule can be determined from the influence of an external electric field, or vice versa for similar systems. Therefore, when compared with existing data, the magnitude of the Stark effect intensity and wavelength change observed for surface TiO−H vibrations on hydroxylated TiO_2 provides information about the electric field causing the changes, and hence acts as a probe for the trapping states involved in creating the electric field.

In our continuing research on TiO_2 photodynamics using diffuse reflectance infrared Fourier transform spectroscopy (DRIFTS), we have characterized photogenerated electrons in deeply trapped states as surface Ti(III)OH moieties with a characteristic stretching frequency, ν(TiO−H), at 3716 cm^{-1}.[6] We have also shown that electrons are able to exist for long times in the free state producing a broad IR absorption proportional to $\lambda^{1.7}$ where λ is the wavelength in microns.[7] We now focus our attention on the shallow electron traps. Occupied shallow electron trapping states are considered necessary for the reduction of oxygen at the TiO_2 surface, but they also facilitate the recombination of charge carriers as shown below.[1]

$$TiO_2 + h\nu \rightarrow e^-_{CB} + h^+_{VB} \quad (1)$$

$$e^-_{CB} \rightarrow e^-_{shallow\ trap} \quad (2)$$

$$e^-_{CB} \rightarrow e^-_{deep\ trap} \quad (3)$$

$$e^-_{shallow\ trap} + O_{2,ads} \rightarrow O_{2,ads}{}^- \quad (4)$$

$$e^-_{trap} + h^+ \rightarrow \text{annihilation} + \text{heat} \quad (5)$$

Despite the fundamental importance of these shallow electron-trapping states, little is known about their physical nature other than the energetic trapping depth and chemical reactivity. In this manuscript, we characterize electrons in shallow traps

* Author to whom correspondence should be addressed.
† Current Address: Department of Chemistry and Biochemistry, Canisius College, Buffalo, NY 14208. E-mail: szczepas@canisius.edu.

10.1021/jp020472v CCC: $22.00
Published on Web 07/16/2002

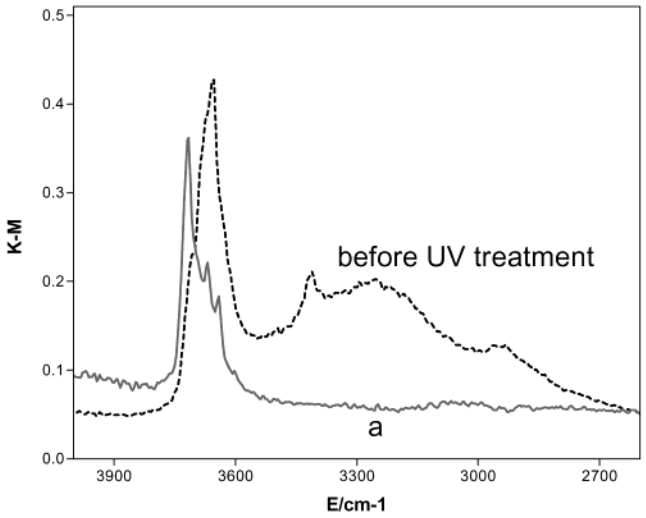

Figure 1. DRIFT spectra of dry TiO_2 that highlight the effects of charge trapping on the stretching vibrations of surface TiO−H bands. Spectrum (a) was acquired following immediate exposure of UV irradiated TiO_2 to O_2 in the dark at 298 K.

according to the delocalized electric field they create, which induces a Stark effect on the surface TiO−H vibrations.

Experimental Section

Commercial, polycrystalline TiO_2 (Degussa P-25, ∼85% anatase, 15% rutile) was purified by sonication in deionized water and recovered by ultracentrifugation before being dried under vacuum. This procedure did not modify DRIFT spectrum peak positions or intensities, but substantially flattened the spectral baseline. O_2 and He gases were dried by passing through P_2O_5 columns.

DRIFT spectra were recorded at 8 cm^{-1} resolution with a Bio-Rad Digilab FTS-45 FTIR spectrometer equipped with an MCT detector and a Spectra-Tech Collector diffuse reflectance accessory installed in the external sampling bench. TiO_2 powders were held in the sample cup of a Spectra-Tech high-temperature environmental chamber (HTEC) that could be resistively heated to 1000 ± 1 K. The chamber could be evacuated to ∼1 μTorr. Gases were introduced through a separate inlet port. UV radiation from a 1 kW Oriel Xe lamp was focused into in the HTEC DRIFT spectra chamber through a KBr window. A 10 cm jacketed water filter removed the IR portion of the radiation. Dynamic temperature control, maintained with a cooled air stream through the coils of the HTEC, prevented excessive heating during the UV treatment and allowed a rapid return to room temperature before analysis. A lens embedded in the compartment lid allowed for irradiation without breaking a zero-air purge. Under typical conditions, irradiation caused the sample temperature to increase to ∼160 °C under vacuum.

Results

Within the time scales of our experiments, irradiation of TiO_2 under vacuum produces trapped holes, and free and trapped electrons. O_2 reacts in the dark with the free and shallow-trapped electrons, leaving only deep-trapped electrons and adsorbed superoxide radicals. A typical DRIFT spectrum of dehydrated TiO_2 before UV treatment is shown in Figure 1. Following irradiation under vacuum, the broad signal from free carriers dominates the spectrum as reported previously.[7] A large band at 3716 cm^{-1}, assigned to ν[Ti(III)O−H] (deep trap)[6] is resolved when the free carriers are removed. This band appears in greatest proportion when the free carriers are quenched in the dark with

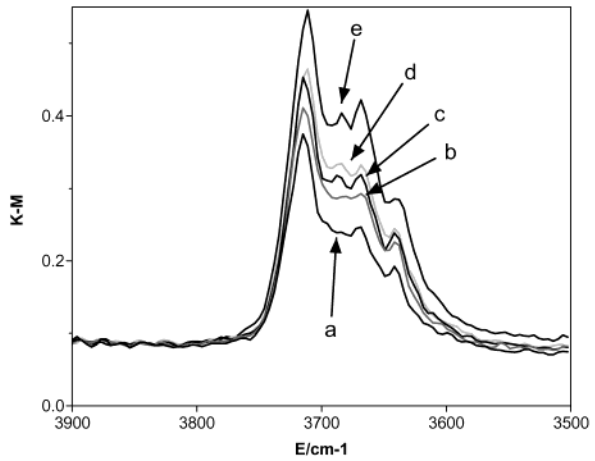

Figure 2. Selected spectra from series acquired during evacuation of HTEC chamber in the dark after irradiation under vacuum followed by addition of O_2. The changes are due to decrease in O_2 pressure from approximately 760 to 10^{-6} Torr. (a) O_2 at ∼760 Torr (Figure 1a). (b−d) Spectra changing upon removal of O_2. (e) O_2 at ∼10^{-6} Torr.

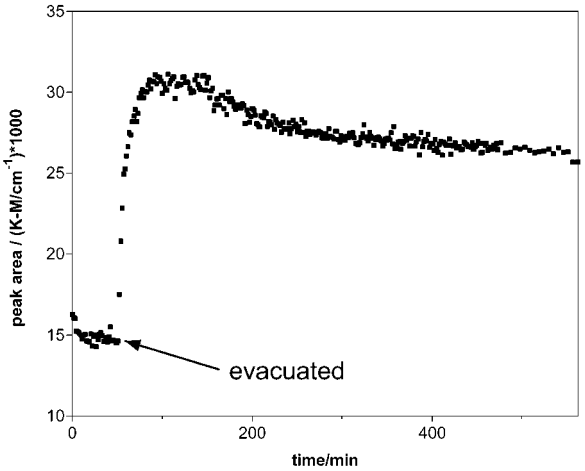

Figure 3. The sum of ν(TiO−H) peak area for all bands as a function of time. Time 0 corresponds to spectrum (a) from Figure 2. The maximum area following O_2 evacuation corresponds to spectrum (e) from Figure 2.

O_2 rather than by self-annihilation. The spectrum following irradiation under vacuum followed by immediate exposure to O_2 is also shown in Figure 1.

Decreasing and eventually removing oxygen causes the adsorbed superoxide to desorb as O_2 following injection of an electron into TiO_2. As the electrons are injected, the total area under all of the ν(TiO−H) bands increases when the headspace O_2 is evacuated as shown in Figure 2. The intensity increase stands out in Figure 3, which shows the total peak area as a function of time, with a clear break upon evacuation. The gradual decrease in peak area after the initial rise is most likely a physical pressure effect, and can be reproduced using He instead of O_2. The initial rise is specific to an O_2-quenched system and will be discussed in the next section. Reintroduction of O_2 during this rise halts the area increase, which resumes upon reevacuation. This sensitivity to O_2 indicates that photogenerated electrons are involved, and that those electrons are populating a shallow trap state in the TiO_2.

Electron trapping in shallow states produces a homogeneous electric field, indicated by the fact that all Ti(IV)O−H stretches are affected equally. Deep traps also produce an electric field, but these fields are localized at the Ti(III)O−H centers. They appear to diminish the field effect of the shallow traps on the

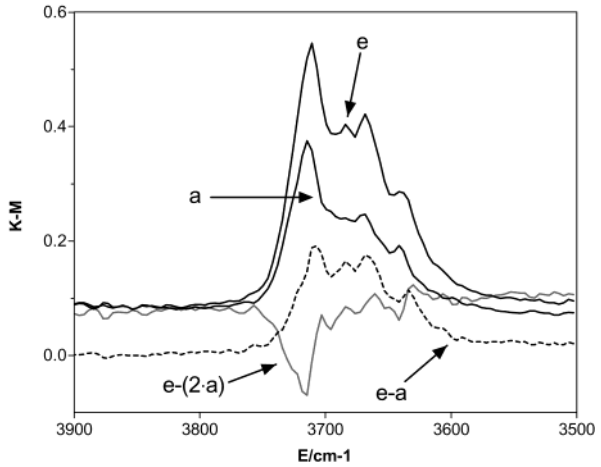

Figure 4. Spectra (a) and (e) from Figure 2 normalized to $Y = 1$ at 3680 cm^{-1} and difference spectrum (e−a). Note that the peak at 3716 cm^{-1} is prominent when all others are subtracted out.

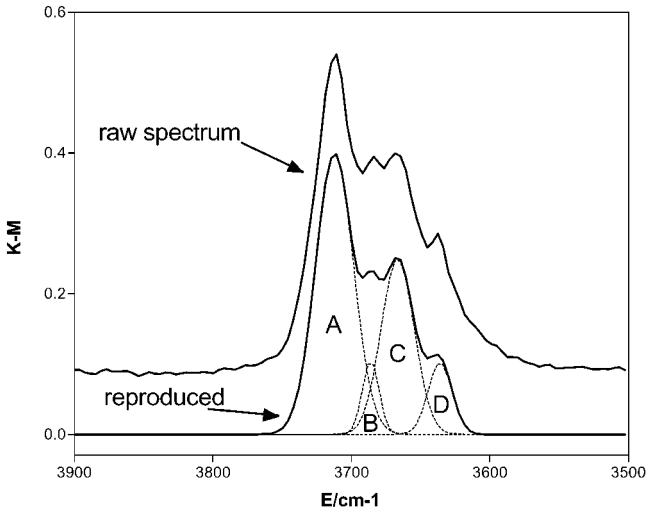

Figure 5. A typical spectrum of TiO−H stretching bands along with Gaussian fits for bands A−D and the resulting spectrum (sum of Gaussian fits) without baseline correction.

3716 cm^{-1} band relative to the other TiO−H stretches. The spectrum obtained by taking the difference between the most and least intense spectra from Figure 2 does not have the same characteristic shape as the parent spectra (Figure 4). When the spectra are scaled vertically to overlay before subtraction, it is clear that the increase is not a simple spectral amplification. The proportional intensity of the 3716 cm^{-1} (deep-trap) band increases less than the other bands.

To investigate differences in the influence of the electric field on Ti(III)O−H and Ti(IV)O−H bands, the spectra were deconvoluted by fitting to four Gaussian curves, using the appearance of distinct peaks among the TiO−H stretching bands as a foundation for spectral peak fitting (Figure 5). The positions of the peak maxima for each Gaussian curve are plotted versus time in Figure 6 to highlight their sensitivity toward the elimination of O_2. A plot of peak area for each fit Gaussian curve versus time is shown in Figure 7. It is clear from Figures 5 and 7 that the spectra are dominated by contributions from peaks A and C, which constitute an average of 82% of the total peak area. While A is relatively well isolated and can be fit with minimal error, peaks B−D are overlapping. As a consequence, the largest area contributor, C, will be assumed to represent the bands in this region of the spectrum. The fraction

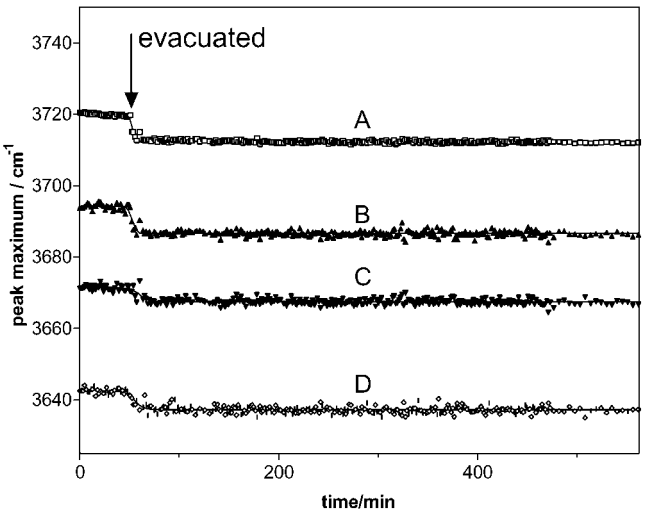

Figure 6. Plot of peak maximum (cm^{-1}) versus time for the Gaussian fits to the spectral series in Figure 2. The sigmiodal fits are included to illustrate the wavelength shift of each fitted band upon the evacuation of O_2.

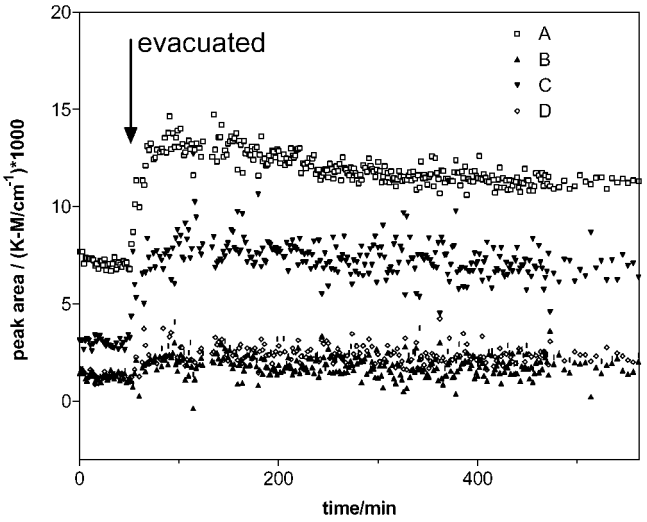

Figure 7. Plot of peak area versus time for the fitted spectra in the series from Figure 2. Note that the areas of peaks B and D are small compared to the scatter in the data.

of the total area for bands A and C is shown in Figure 8. It is clear that the area of peak A responds differently from peak C upon evacuation. In a similar fashion, the full-widths at half-maximum (fwhm) for these Gaussian curves are plotted versus time in Figure 9, showing a strong dependence for band A, but no clear change for band C.

Discussion

The Stark effect, observed upon removing oxygen, is manifested as a band energy and intensity change for ν(TiO−H). It is caused by an electric field due to occupied shallow electron traps. After initial irradiation in vacuo, introduction of O_2 in the absence of UV causes the signal from the free electrons[7] to disappear, most likely due to the formation of O_2^-(ads).[8] A band for $\nu(O_2-H)$ is not observed in the IR because O_2^- (aqueous $pK_a = 4.8$)[9] is not extensively protonated. The single-step reverse reaction causes the surfacial O_2^- to lose an electron back to TiO_2 and escape as O_2(g). As expected, there is no evidence of these electrons in the conduction band,[7] which lies at a high potential. The electrons must therefore be injected into lower-lying trap states.[10] The charge injection alters the

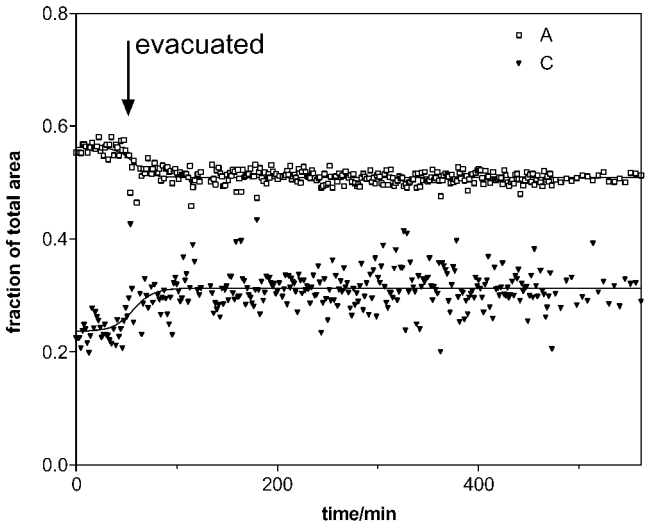

Figure 8. Plot of fraction of the total ν(TiO−H) peak area versus time for peaks A and C from the fit spectra in the series from Figure 2. The small contributions from peaks B and D are not shown. The sigmiodal fits are included to illustrate the relative influence of each fitted band on the total area upon the evacuation of O_2.

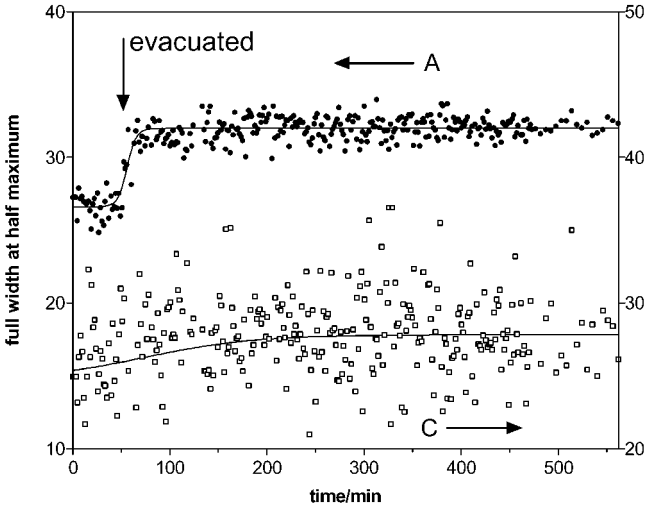

Figure 9. Plot of fwhm versus time for the fit spectra in the series from Figure 2 along with the sigmiodal fits. Note that peak A shows a clear dependence on the evacuation event, but peak C does not.

electric field, leading to the ν(TiO−H) intensity increases observed when the O_2-quenched system is evacuated. In a previous paper, we showed that Ti(III)OH formed upon reduction of acidic Ti(IV)OH sites, resulting in a shift of ν(TiO−H) from 3647 to 3716 cm^{-1} and an increase in intensity (Figure 1).[6] Using ab initio data presented by Hermansson for the influence of an electric field on the DO−H vibration,[11] this shift corresponds to an electric field strength change from +0.044 au to 0.033 au. This shift directly supports the assignment of these bands to a single titanol structure type with titanium in either the +4 or +3 form (i.e., Ti(III/IV)O−H).

The observation of Stark effects for both Ti(III) and Ti(IV) centers indicates that the electric field arises from a diffuse state. When the electric field is directed along the bond axis, the wavelength and intensity shifts are approximately proportional, and exhibit a maximum whose position is sensitive to the bond polarity. However, when the bond angles change, as in the present case, the two effects clearly do not remain linear. Considering first the individual responses, the magnitude of the Stark shift of the vibrational state energy is the same for Ti(III) and Ti(IV) centers, but with a different shift in intensity as well as fwhm. When considered from a structural point of view, a static negative field is expected to contract the equilibrium bond lengths and bond angles of surface TiO−H groups as shown in Figure 10 for neutral hydroxylated TiO_2. As the bond lengths and angles contract, the energies and intensities of the vibrational frequencies change, as shown in Figure 6. Under some conditions, this can affect the very nature of the transitions involved in these vibrations (Figures 3 and 7).

The similar wavelength change observed for Ti(III)O−H and Ti(IV)O−H stretches indicates a similar potential energy change for both surface moieties. The energy of the bond length compression is nearly equivalent, but the magnitude of the displacement is different for Ti(III)O−H and Ti(IV)O−H. Because the Ti(III)O−H bond is already compressed with respect to the Ti(IV)O−H bond, an equivalent potential change is manifested in a smaller displacement.

The same argument can be used to explain the difference in the band intensity response to the electric field. The Ti(IV)O−H bond is slightly lengthened from its optimal orientation by the steric influence of the surface. Bond compression improves the orbital overlap, and the intensity of the vibration increases due to a higher density of available states. However, the Ti(III)O−H bond is already shortened, so further compression is not as beneficial for its orbital overlap. The nature of the Ti(III)O−H vibrational transition changes slightly as a consequence of this high level of distortion, leading to band broadening. This suggests that the bond angle change for Ti(IV)O−H produces less change in the nature of the transition than for Ti(III)O−H, as indicated by the change in the fwhm.

Because the Stark effect from shallow electron trapping is observed for both Ti(III)O−H and Ti(IV)O−H vibrations, the electric field due to electrons in shallow traps is apparently homogeneous (Figure 2). In contrast, deep electron trapping appears to affect only one titanol stretching band. Because all TiO−H stretches are equally affected (Figure 4), the shallow traps must be either localized at every titanol, or delocalized to affect all the titanol functionalities equally. A delocalized trap structure is supported by the influence on the band known to arise from Ti(III)O−H stretches.[6] The shallow state must be displaced from the titania centers in order to influence both Ti(IV)O−H and Ti(III)O−H type stretches, since the latter is

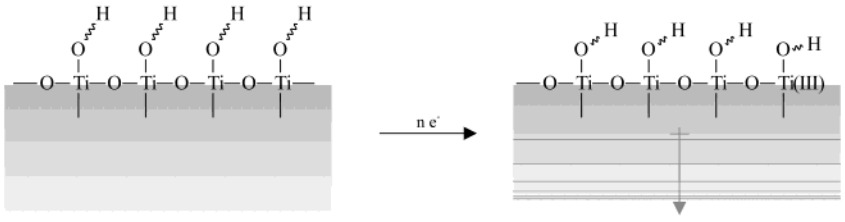

Figure 10. Diagram illustrating the relative influence of localized and diffuse electric fields on the bond lengths and angles of surface TiO−H bonds.

unlikely to accept additional charge. The observations presented above are explained by an equivalent field strength acting on both the Ti(III)O−H and Ti(IV)O−H vibrations, resulting in similar wavelength changes.

In light of these observations, we propose that the physical nature of the shallow electron traps corresponds to delocalized electrons coupled with two-dimensional lattice phonons. This is similar to the two-dimensional charge traps proposed for CdSe.[12] Free conduction band electrons are coupled with the bulk lattice phonons in order to conserve momentum in TiO_2.[13] Localization of a electron on at Ti(IV) center causes the surrounding lattice to distort and create a net polarization to compensate for the negative charge. The combined state of the electron and the distortion cloud behaves as a single quasiparticle called a small polaron.[14] The physical motion of the lattice (phonons) required to translate such a polaron gives rise to the IR spectral signature for free conduction band electrons.[7] However, this coupling with the lattice is not possible as the electrons approach the surface. It is likely that the electrons switch to coupling with two-dimensional surface phonons, which have been observed on anatase surfaces.[15] This coupling forces the electrons to occupy a two-dimensional state delocalized across the surface. Therefore, the fundamental distinction between the free state and the shallow traps is that electrons in the free state are coupled with bulk phonons and are mobile in three dimensions, and electrons in shallow traps are confined to the two-dimensional surface.

The identification of the shallow electron trapping state as a two-dimensional delocalized surface state is in agreement with much of the published data regarding TiO_2 properties and photoreactivity. The lack of a previous structural assignment to the shallow electron traps may be due to their delocalized nature. In addition, the super-wettability of the TiO_2 surface, obtained by irradiation, occurs through the formation of a checkerboard of hydrophilic and hydrophobic domains on the surface on the scale of ∼50 nanometers.[16] This requires the influence of trapped charges to be transmitted across dimensions about 2 orders of magnitude larger than the unit cells, far beyond molecular-scale interactions, but in accord with two-dimensional polaron states.[17] The energetic depths of the shallow electron traps, which have been assigned in a range around 0.5 eV below the CB edge,[18] would be sensitive to the nature of the 2-dimensional coupling. Because different crystal surfaces have different surface phonon modes,[15] they should be expected to support distinct electron trapping depths. This may account for the anisotropy in reduction rates observed on different cleavage surfaces for photoactivated rutile TiO_2.[19] Competing reduction reactions with specific surface-dependent rates could help explain the wide range of limiting efficiencies observed for different types of TiO_2 photocatalysts.[20]

Conclusions

We have shown that the intensities of surface hydroxyl stretching bands are sensitive to electric fields caused by trapped charge carriers. Using these intensity changes as a reference, we observe reversible electron abstraction from TiO_2 by O_2. We also show that the reverse reaction injects electrons to shallow trapping states, which appear to be delocalized across the surface. The assignment of this shallow electron-trapping structure corresponds well with available literature data.

Acknowledgment. This work was funded by NSF (Grant # BES-9619885 and by DARPA through the Northrop-Grumman Corp.

References and Notes

(1) Martin, S. T.; Chio, W.; Hoffmann, M. R. *Chem. Rev.* **1995**, *95*, 69−96.
(2) Norris, D. J.; Sacra, A.; Murray, C. B.; Bawendi, M. G. *Phys. Rev. Lett.* **1994**, *72*, 2612.
(3) Komoda, Y.; Rao, T. N.; Fujishima, A. *Langmuir* **1997**, *13*, 1371.
(4) Zaban, A.; Meier, A.; Gregg, B. A. *J. Phys. Chem. B* **1997**, *101*, 7985.
(5) Ai, X. C.; Jin, R.; Ge, C. B.; Wang, J. J.; Zou, Y. H.; Zhou, X. W.; Xiao, X. R. *J. Chem. Phys.* **1997**, *106*, 3387.
(6) Szczepankiewicz, S. H.; Colussi, A. J.; Hoffmann, M. R. *J. Phys. Chem. B* **2000**, *104*, 9842.
(7) Szczepankiewicz, S. H.; Moss, J. A.; Hoffmann, M. R. *J. Phys. Chem. B* **2002**, *106*, 2922.
(8) Ishibashi, K.; Fujishima, A.; Watanabe, T.; Hashimoto, K. *J. Phys. Chem. B* **2000**, *104*, 4934.
(9) Buxton, G.; Greenstock, C.; Helman ,W.; Ross, A. *J. Phys. Chem. Ref. Data* **1988**, *17*, 513.
(10) Ishibashi, K.; Nosaka, Y.; Hashimoto, K.; Fujishima, A. *J. Phys. Chem. B* **1998**, *102*, 2117.
(11) Hermansson, K. *J. Chem. Phys.* **1993**, *99*, 861.
(12) Bawendi, M. G.; Carroll, P. J.; Wilson ,W. L.; Brus, L. E. *J. Chem. Phys.* **1992**, *96*, 946.
(13) Pankove, J. I. *Optical Processes in Semiconductors*; Dover: New York, 1975.
(14) Eliot, S. R. *The Physics and Chemistry of Solids*; John Wiley and Sons: Chichester, 1998.
(15) Durinck, G., Poelman, H.; Clauws, P.; Fiermans, L.; Vennik, J.; Dalmai, G. *Solid State Commun.* **1991**, *80*, 579.
(16) Wang, R.; Hashimoto, K.; Fujishima, A.; Chikuni, M.; Kojima, E.; Kitamura, A.; Shimohigoshi, M.; Watanabe, T. *Adv. Mater.* **1998** *10*, 135.
(17) Sumi, H.; Sumi, A. *Solid State Commun.* **1991**, *78*, 883.
(18) For example: (a) Weng, Y. X.; Wang, Y. Q.; Asbury, J. B.; Ghosh, H. N.; Lian, T. *J. Phys. Chem. B* **2000**, *104*, 93−104. (b) Boschloo, G.; Fitzmaurice, D. *J. Phys. Chem. B* **1999**, *103*, 2228. (c) Boschloo, G.; Goosens, A. *J. Phys. Chem. B* **1996**, *100*, 19489.
(19) Lowekamp, J. B.; Rohrer, G. S.; Hotsenpiller, P. A. M.; Bolt, J. D.; Farneth, W. E. *J. Phys. Chem. B* **1998**, *102*, 7323.
(20) For example: Herrmann, J. M.; Tahiri, H.; Guillard, C.; Pichat, P. *Catal. Today* **1999**, *54*, 131.